

Study of Correlations between Microstructure and Conductivity in a Thermoplastic Polyurethane Electrolyte

C. A. Furtado

Centro de Desenvolvimento da Tecnologia Nuclear—CDTN/CNEN, CP 941, 30123-970, Belo Horizonte, MG, Brazil

G. Goulart Silva* and J. C. Machado

UFMG/ICEx/Departamento de Química, CP 702, 31270-901, Belo Horizonte, MG, Brazil

M. A. Pimenta and R. A. Silva

UFMG/ICEx/Departamento de Física, CP 702, 30123-970, Belo Horizonte, MG, Brazil

Received: December 3, 1998; In Final Form: May 5, 1999

Micro-Raman and positron annihilation lifetime spectroscopy (PALS) have been used to investigate the structure of a thermoplastic polyurethane/LiClO₄ solid flexible polymer electrolyte at room temperature. Correlation between the free volume and carrier concentration with ionic conductivity was observed. The polyurethane soft phase consisted of a poly(tetramethylene glycol-co-ethylene glycol) copolymer reinforced by condensation with hexamethyldiisocyanate. The range of salt concentration between 5 and 35 wt %, which attained the beginning of phase segregation, was also studied by differential scanning calorimetry (DSC), which showed the presence of three thermal events; the soft-phase T_g , a change in heat capacity suggested as the hard-phase T_g , and a hard-phase ordering endotherm. The total ionic conductivity was found to be approximately $4 \times 10^{-6} \text{ S cm}^{-1}$ at 23 °C up to 27 wt % salt, whereas there were pronounced changes observed by the spectroscopic techniques. The PALS measurements indicated a decrease of 40% of the ratio $(V_{f3}/(V_{f3})_0)$ between the free volume parameters probed by the positron particle. This ratio is proportional to the fractional free volume of the system. The micro-Raman results showed an increase of ionic aggregation, although the charge carrier concentration increased significantly in the range of compositions studied. The opposite effects of the microstructural changes and the maximum conductivity value, in the observed range of concentrations, are discussed.

Introduction

The use of macromolecular materials as electrolytes in solid-state, room-temperature electrochemical devices^{1–4} motivates the study of ionic dissociation and transport phenomena in polymer/salt binary systems. Earlier investigations of the structural properties and conduction mechanism of these electrolyte systems have indicated that the ionic conduction occurs in the amorphous phase of the material⁵ and, therefore, it depends on the macromolecular chain dynamics (increasing flexibility and free volume density imply increasing conductivity) and the degree of ionic aggregation. Consequently, with the aim of enhancing ionic conductivity, efforts have been made to obtain molecular polymeric matrixes with reduced crystallinity, high solvating power, and low glass transition temperature. Poly(ethylene oxide) (PEO) is the reference polymer for ionic conduction, since it is the best host matrix for inorganic salts.⁶ However, alternative systems have been investigated, including the preparation of polyurethane (PU) networks or thermoplastics.^{7–15} Ligand agents, such as urethane nodes —NHCOO— (hard phase), condense with polyether macromonomers (soft phase) in diblock long chains, with high amorphous character. This phase-segregated morphology is not favorable to the existence of long polyether sequences, avoiding

high ordering chains. On the other hand, it promotes hydrogen bonding within the hard domain on adjacent polymer chain segments and of the hard domain with the polyether, resulting in polymers with a good dimensional stability. The reaction between multifunctional compounds allows the formation of networks and prevents the material from creeping.¹⁶

Polyurethane network electrolytes were first proposed by Le Nest and co-workers.^{7,8} The authors investigated a broad set of polyurethanes based on various types of polyethers. Values of conductivity close to $10^{-5} \text{ S cm}^{-1}$ were attained for the best materials at room temperature. However, low values of the cationic transport number (± 0.02) were considered as the main drawbacks for application purposes.⁸ More recently, PU network electrolytes have been studied with the aim of correlating ionic conductivity with the free volume size and concentration. Two types of systems have been explored: the poly(ether urethane) (PEU) electrolytes^{17,18} and plasticized PEU.^{10,19} Positron annihilation lifetime spectroscopy is able to measure free volume properties directly and will be employed in the present work to study a thermoplastic PU.

The interest in using thermoplastic polyurethane (TPU) as matrix for polymer electrolytes is related to the possibility of increasing the mechanical strength of linear polyethers, avoiding rigid covalent cross-linking, by means of obtaining a phase-separated microstructure in which the hard segment works as a “hard filler”. Watanabe et al.¹¹ investigated the morphology and

* Corresponding author. Phone: 00 55 31 499 5768. Fax: 00 55 31 499 5700. E-mail: glaura@dedalus.lcc.ufmg.br.

ionic conductivity of electrolytes prepared from polyether poly-(urethane urea) (PEUU) based on poly(propylene oxide) (PPO) and LiClO₄. PEUU formed a two-phase structure, with a PPO phase and a poly(urethane urea) phase. A concentration of 30% of hard segments was used in order to make a continuous PPO phase conduction path. LiClO₄ was selectively dissolved in the PPO phase. This system exhibited low conductivities of 10⁻⁸ S cm⁻¹ at 40 °C, and the conductivity isotherms did not show a pronounced dependence with salt concentration.

Mc Lennaghan et al.^{13,20} have studied a TPU based on poly-(ethylene glycol) (PEG), 4,4'-diphenylmethanediisocyanate (MDI), and 1,4-butanediol (BDO), which are used to prepare hosts for alkali metal salts which have a high degree of phase separation. The authors evaluated a range of hard domain concentration from 22% to 76%. Variations of T_g between -39 and 14 °C were determined for electrolytes prepared with a PEG 1000. They observed that the best performance is achieved by the phase-separated TPU with the lowest hard domain concentration (22%), in which a conductivity greater than 10⁻⁶ S cm⁻¹ was obtained at room temperature for a LiClO₄ electrolyte with 10 wt % of salt. They concluded that the ionic conductivity is sensitive to the phase-separated nature and a lower T_g of the soft segment leads to a higher conductivity. A maximum was observed in the conductivity isotherms for electrolytes with 10 wt % of LiClO₄ followed by a decrease of 3 orders of magnitude up to 40 wt % of salt.

Seki et al.,¹² studying a commercial PU based on poly-(tetramethylene glycol)(PTMG)/MDI/BDO, obtained conductivities between 10⁻⁷ and 10⁻⁶ S cm⁻¹ when the LiClO₄ content increased between 3 and 13 wt %. Both Seki et al.¹² and Mc Lennaghan et al.^{13,20} have shown that a higher temperature endothermic transition observed in the TPU disappeared with the addition of ionic salt.

The work of van Heumen and Stevens¹⁴ also showed loss of long-range ordering of the hard domain with salt concentration increase when studying a PTMG/MDI/BDO TPU. Increases of the hard segment T_g were observed for systems with LiCF₃SO₃ and Li(CF₃SO₂)₂N¹⁴ and with NH₄CF₃SO₃.¹⁵ Their FTIR study suggested interaction of the lithium cation with the TPU hard segment.¹⁴ Contrary to Mc Lennaghan et al.,^{13,20} a maximum conductivity is not observed as a function of concentration in their isothermal studies.^{14,15}

Ferry et al.⁹ have carried out a spectroscopic investigation of TPU electrolytes by Raman and IR spectroscopy. They also studied a commercial TPU based on PTMG/MDI/BDO, in this case with LiClO₄ additions up to 21 wt %. Very low values of conductivity ($\approx 10^{-9}$ S cm⁻¹) were obtained at room temperature, probably associated with a high content of hard segments which were not discussed. The conductivity isotherms did not show a maximum at a particular concentration up to 21 wt % of salt. Their results suggest a competition between hydrogen bond and lithium cation coordination, especially in the hard segments of the host polymer. Relative amounts of different ionic species were determined by fitting the Raman bands in a similar way to that which will be described in this work. "Free" anions (observed with the 932 cm⁻¹ line) were present in concentrations between 50% and 35% of the total anionic species when LiClO₄ concentration increased from 1 to 21 wt %. Contact ion pairs (939 cm⁻¹) and aggregates (946 cm⁻¹) increase in the same range of salt concentration between $\sim 35\%$ and 42% and ~ 17 and 22%, respectively.

This paper focuses on the systematic investigation of the effects of LiClO₄ concentration on the structure and bulk impedance of a linear polyurethane synthesized with poly-

(tetramethylene glycol-co-ethylene glycol) PTMG/PEG poly-ether. Characterization of the system was carried out by using thermogravimetry (TG), differential scanning calorimetry (DSC), Raman spectroscopy, and positron annihilation lifetime spectroscopy (PALS). TG was used to investigate the thermal stability and drying behavior. DSC has been extensively used to study the phase transitions of polymer electrolytes in order to correlate the crystalline and amorphous thermodynamic parameters with the conductivity behavior.²¹ In the case of a phase-separated polyurethane, this study includes the analysis of soft and hard segments events.^{9,14}

The Raman technique has proven to be a valuable tool to investigate ionic association and complex formation in electrolyte polymers.²²⁻²⁴ The study of intense symmetric stretching of anions ClO₄⁻ can be accessed through Lorentzian fitting of the band splitting, thus obtaining an evaluation of the various ionic associations. Micro-Raman spectroscopy permits the determinations of phase separation over a small scale.²⁵

The main goal of the correlation between conductivity and microstructure features can be easily understood with the analysis of the VTF equation, which in general fits the typical curvature of conductivity as a function of temperature:

$$\sigma = A[\exp -B/R(T - T_0)] \quad (1)$$

In a free-volume model, the VTF parameter B can be equated to $(\gamma v^*/v_f)$, where v_f is the average free-volume per particle, v^* is the critical volume of a void required to transport, and γ is a constant that allows the overlap of the free volume. It should be noted that B is a function of expansivity. Souquet et al.²⁶ have shown that B obtained from the fitting of conductivity versus temperature variations is approximately 0.1 eV for several polymer electrolyte systems. This result allows the calculation of a critical free volume of 30 Å³, using approximate values for the parameters included in B .²⁶ The parameter A can be deduced from gas kinetic theory or from the harmonic oscillator model.²⁶ Nevertheless, A is directly proportional to the concentration of the species that provides ionic conductivity which could be "free" cations and anions as well as ion pairs and higher clusters.²⁷ The free-volume model has been at the same time extensively used and criticized. The main criticism has pointed out the weakness of using this equation to correlate the conductivity results with the system features, as with the polymer/salt structure and dynamics. Some authors have pursued the correlation between the ionic conductivity and structure using PALS^{17,18} or vibrational spectroscopy.^{9,24} The purpose of the present work is to investigate this kind of correlation with an evaluation of the behavior at room temperature, when the nominal salt concentration is increased. On one hand, some insight about the evolution of the concentration of carriers may be obtained with the Raman study, as discussed above. On the other hand, PALS is the preferred technique to study the free-volume features.

PALS has drawn extensive interest in the polymer field due to the possibility of obtaining direct information about the dimension and relative concentration of static and dynamic free-volume holes in amorphous materials.^{17,18,28-31} This technique uses the ortho-positronium (o-Ps, triplet state) lifetime, τ_3 , as an indication of the local electron density and the inter- and intramolecular mean free volume cavity radius. The o-Ps intensity, I_3 , reflects the probability of o-Ps formation and the relative concentration of free-volume cavities in the material.

The mean free volume of the material can be estimated empirically by assuming a specific void cavity shape. For free-volume sites modeled as spherical cavities, τ_3 is directly related

to the radius of this free volume.^{28,32,33} As the size of the free-volume cavity increases, the local electron density surrounding the o-Ps decreases, and thus o-Ps has a slower annihilation rate or longer lifetime (τ_3).

This paper examines the correlation between static and dynamic parameters given by the Raman and PALS spectroscopic analysis and the ionic conductivity obtained by impedance spectroscopy at room temperature when the LiClO₄ concentration is raised. The thermoplastic polyurethane morphology is also studied by DSC to help establish a complete picture of the system.

Experimental Details

Thermoplastic polyurethanes were obtained using PTMG/PEG as the soft segment and the hexamethyldiisocyanate (HMDI) as hard segment. The macromonomer was chosen by following our previous comparative study of the PTMG and PTMG/PEG liquid electrolytes.³⁴ The copolymer exhibits the best conductivities associated with the lowest association and tendency to crystallize. The choice of the HMDI was made in an attempt to prepare a TPU which avoids possible influences of aromatic content in the hard phase.

Membranes were synthesized by mixing stoichiometric amounts^{35–37} of HMDI and PTMG/PEG in CH₂Cl₂ at room temperature under N₂ atmosphere in the presence of small amounts (0.1 mL/10 g polyether) of dibutyltin dilaurate as a catalyst. The concentration of the reagents in the solution was 0.07 mol/L, sufficiently low to allow a constant stirring. After mixing, the reaction solution was poured in a plate. The solvent was then removed under vacuum in an oven at 60 °C for 2 days. Transparent, visually elastic, and resistant membranes were obtained after about 25 h of reaction. The concentration of hard segments in the TPU was kept at 17%.

The copolymer composition, as estimated by ¹H NMR analysis, was 65% of PTMG and 35% of PEG, in weight. ¹H NMR spectra were obtained with a 200 MHz Bruker Avance DPX200.

The GPC measurements were carried out using a Shimadzu LC-10AD/CTA-10A GPC, equipped with a differential refractometer RID-6A. The solvent (THF) was eluted (1 mL/min) through two Shim-pack columns (805/804, ideal range of separation up to 10⁶ g/mol) at 40 °C. The results of the GPC were: PTMG/PEG–Mn = 880, *I* = 1.8 and PU(PTMG/PEG)–Mn = 77000, *I* = 1.7.

Solutions in the concentration range between 1 and 35 wt % of LiClO₄ were prepared by dissolving both salt and polymer in a 1:1 mixture of tetrahydrofuran and dichloromethane. Films were obtained by casting this solution in Petri dishes and removing the solvent slowly at ambient pressure, followed by vacuum (~10⁻³ Torr) evaporation for 48 h at 60 °C. The films were transparent and homogeneous until the composition of 22 wt %. At higher concentrations, macroscopic phase segregation was observed. The samples were stored in a desiccator and, prior to any conductivity or spectroscopic measurement, were again carefully dried for around 24 h at 60 °C under reduced pressure (~10⁻³ Torr) to ensure that no absorbed water was present.

TG analysis was performed using a TA Instruments SDT 2960 Simultaneous DTA–TGA instrument with a scan rate of 10 °C/min until 600 °C, under N₂ atmosphere. TG data were used to confirm that the DSC thermal events, which will be shown later, are really phase transitions rather than associated with any weight loss. Moreover, the thermal stability study is also useful for further application in technological devices.

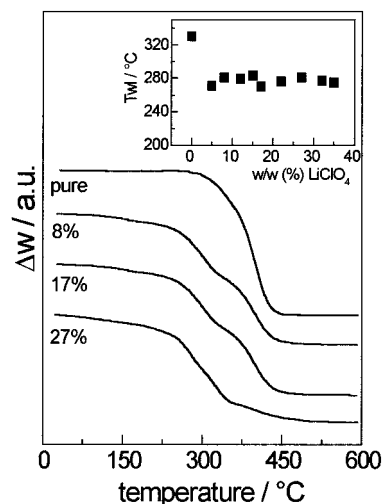


Figure 1. Typical TG curves (10 °C/min., N₂) obtained for the PU-(PTMG/PEG)/LiClO₄. Salt concentration is indicated in the figure. Inset shows the initial weight loss temperature (T_{wi}) as a function of the salt concentration.

Typical TG curves for the PU/LiClO₄ system are shown in Figure 1 in which are also indicated the overall values of the initial thermal degradation temperature (T_{wi}) when the concentration is increased. As can be seen from Figure 1, the pure polymer decomposes in a single step beginning at 330 °C. The introduction of the salt promotes the creation of a second stage which reflects the salt/polymer complex degradation, beginning at 275–285 °C. This behavior may be explained by the weakness of the C–O bond, caused by the electronic density decreasing due to the O–Li⁺ interaction.

DSC measurements were carried out with a TA Instruments 2920 DSC, in two scanning experiments: 25 to 150 °C and –120 to 200 °C, at heating rates of 10 °C/min; after the first heating run an annealing of 3 min at 150 °C was undertaken. The cooling stage was performed with a quenching in the DSC cell, with a cooling rate of approximately 40 °C/min. Samples were sealed in aluminum DSC pans, with the sample mass ranging from 3 to 5 mg, and measurements were performed under He atmosphere. DSC curves showed for comparison in this work, as well as TG curves, were scaled with the sample weight. The transition (T_g , T_m) values are quoted as the extrapolated onset: the intersection of the baseline and the departure from baseline upon heating as the transition begins. The accuracy of the transition temperatures determined was typically of ± 1 °C. In cases of very broad T_g 's, the error can be as high as ± 2 °C.

Raman spectra were recorded in a triple monochromator spectrometer (Dilor XY) equipped with a multiarray detector (Gold). A microscope (Olympus BH-2) was coupled to the spectrometer, allowing a Raman analysis with spatial resolution of about 1 μ m (micro-Raman technique). An argon laser was used (Coherent Innova 70) operating in the green line ($\lambda = 514.5$ nm) with power of 100 mW.

PALS measurements were performed using a fast–fast coincidence system (ORTEC) with time resolution of 280 ps, given by the ⁶⁰Co prompt curve. The ²²Na positron source with approximately 4×10^5 Bq activity was sandwiched by two 3.5 μ m thick foils of Mylar. The source correction was approximately 10%. The lifetime spectra were resolved in three components with the POSITRONFIT-EXTENDED program.³⁸ For the obtained lifetimes, τ_i , and associated intensities, I_i , the subscripts 1, 2, and 3 refer to para-positronium (p-Ps), free

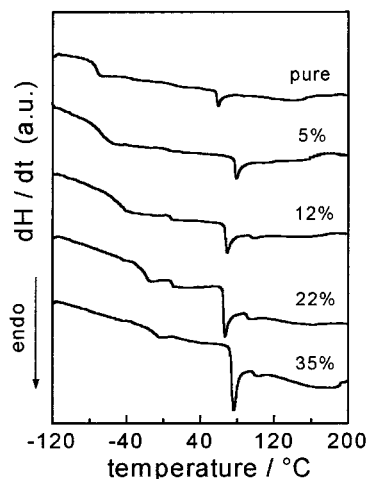


Figure 2. Typical DSC curves obtained for the PU(PMTG/PEG)/LiClO₄. Salt concentration is indicated in the figure.

TABLE 1: Temperatures of the Phase Transitions Determined for the PU(PMTG/PEG)/LiClO₄ System^a

wt % LiClO ₄	$T_{g1}/^{\circ}\text{C}$	$T_{g2}/^{\circ}\text{C}$	$T_3/^{\circ}\text{C}$	$\Delta H_{T_3}/\text{J g}^{-1}$
0	-78	5	57	2
5	-79	5	76	3
8	-63	4	78	3
12	-64	6	66	3
15	-53	-	71	3
17	-41	7	77	3
22	-28	8	64	4
27	-21	8	61	5
32	-20	8	55	11
35	-15	11	73	30

^a Accuracy of temperature determinations is $\pm 1^{\circ}\text{C}$.

positron, and ortho-positronium (o-Ps), respectively. The experimental deviations of τ_3 and I_3 are ± 0.05 ns and $\pm 1\%$, respectively. The samples were measured on about 1.5 mm thick cast polymer sheets at 21 $^{\circ}\text{C}$.

The total ionic conductivity was measured with a Hewlett-Packard 4192A electrochemical impedance spectrometer. The films were sandwiched by two stainless steel electrodes. The frequency range used was 10–10⁵ Hz with an amplitude of 50–80 mV.

Results and Discussion

Phase Transitions. Figure 2 shows typical DSC curves obtained for the PU(PMTG/PEG)/LiClO₄ system, corresponding to the second heating experiments. These curves show that the TPU studied presents three thermal events: a low-temperature soft-segment T_g , a heat capacity change near 5 $^{\circ}\text{C}$, which may be attributed to the aliphatic hard-segment T_g , and an ordering endotherm near 60 $^{\circ}\text{C}$. The temperature observed for these thermal events changes with increasing concentration as shown in Table 1.

Several authors have studied the TPU thermal behavior by DSC.^{13,40,41} Leung and Koberstein,⁴⁰ for example, showed the increase of the soft segment T_g from near -80°C up to 30 $^{\circ}\text{C}$ when the TPU hard-segment content increases to 80 wt %. They reported a detailed study by SAXS and DSC of a PPO/MDI/BD system upon various annealing treatments. The T_g of the aromatic hard segment is found around 100 $^{\circ}\text{C}$ for TPU with more than 30 wt % of hard segment. They observed also for these hard-segment concentrated TPU's the influence of several annealing treatments upon the high-temperature endotherms. TPU's systems with less than 30 wt % of hard segment

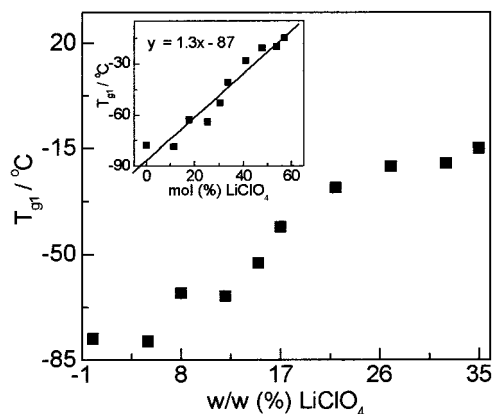


Figure 3. Glass transition temperature of the soft segment versus salt concentration.

TABLE 2: Comparison of the T_g Variation with Concentration for Polymer/Salt Systems

system	$\delta T_g/\delta X_{\text{sal}} (^{\circ}\text{C}/\text{mol } \%)$
PU(PMTG/PEG)/LiClO ₄	1.3
PU(PEG-22% hard seg.)/LiClO ₄ ^a	3.3
P(EPI-OE)/LiClO ₄ ^b	2.1
PU(EPI-OE-AGE)/LiClO ₄ ^b	2.5
POE/LiClO ₄ ^b	4.2
POE/LiCF ₃ SO ₃ ^b	2.8

^a Reference 13. ^b Reference 39.

previously reported^{13,41} do not show high-temperature ($\geq 100^{\circ}\text{C}$) endotherms, which is the case of the PU(PMTG/PEG) system studied in this work.

The first thermal event observed in Figure 2 is the change in heat capacity of the soft-segment glass transition (T_{g1}) in polyurethanes.^{13,39,40,41} The polyethers forming the soft segment present T_g 's well below room temperature.^{21,39} The macromonomer used to synthesize the TPU in this work was previously studied,³⁴ and the T_g values ranged between -87°C for the pure polymer and -70°C for the sample with 32 w/w (%) of salt. The obtained value at -78°C for the TPU pure polymer is significantly lower than other values found in the literature. For example, the TPU based on PEG ($M \approx 1000$), with a concentration of 22% of hard segment, gives a T_{g1} of -39°C .¹³ Another polyurethane based in PTMG homopolymer shows $T_{g1} = -44^{\circ}\text{C}$.⁹ The lower value of T_{g1} indicates a high flexibility of the soft segment. In the present case, the low concentration of the hard segment (17%) and their aliphatic nature do not produce a high increase in the polyether T_g .

As shown in Figure 3 and Table 1, the introduction of the salt in the polymer matrix leads to an increase of T_{g1} with increasing salt concentration up to about 22 wt % of salt, indicating a stiffening of the chain due to the ion-dipole interaction between the cation and the oxygens of the polyether. Above this composition, T_{g1} values tend toward a plateau. The T_{g1} versus salt concentration showed a slope of 1.3 $^{\circ}\text{C}/\text{mol } \%$, obtained by using T_g from all samples on a least-squares linear fit. A similar value is obtained if the T_g 's for the samples with higher concentration than 22 wt % are not taken into account. This value is significantly lower than those found for other systems,³⁹ as shown in Table 2. This is an important result obtained for the prepared TPU. If the amorphous phase associated with the soft segment retains a lower T_g when high concentrations of salt are added, this will probably have a beneficial influence in retaining a favorable structure relative to the ion displacement via solvation/dessolvation in the polyether segments.

The second thermal event, equally a change in C_p without associated heat transfer, may be attributed to a glass transition (T_{g2}) of the aliphatic low-concentration (17%) hard segment. This attribution is proposed by similarity with the observed T_g of the hard segment in the MDI-based TPU's.⁴⁰ This event is better defined, showing a higher change in heat capacity through the transition, with salt introduction. As suggested by other authors,^{9,14} the Li^+ ions compete with the hydrogen bonds in the hard segments, and this new interaction could be responsible for the increase in ΔC_p through the transition. The temperature T_{g2} does not change significantly with the composition of the PU(PTMG/PEG)/ LiClO_4 system, as shown in Table 1, exhibiting just a small increase after 22 wt %.

The third thermal event, at approximately 57 °C for the pure polymer, may be attributed to an endothermic process, with an associated relaxation, showing a heat capacity (ΔC_p) change. This phenomenon may be due to a loss of order close to the hard domain involving hydrogen bond dissociation. In the case of polyurethane with low concentration of hard domains (about 20%), involving low molar mass (~ 1000) polyethers, some examples are found in the literature, indicating the presence of a single endotherm for temperatures between 80–90 °C.^{13,40,41} This endotherm was initially interpreted as being associated with hydrogen bond dissociation, but later it was discussed in terms of morphological behavior.^{41–43} In the latter case, it was proposed that the hydrocarbon chains of the hard segments would be responsible for the observed ordering, not involving hydrogen bonding.

As shown in Table 1, the introduction of LiClO_4 to the PU(PTMG/PEG) polymer matrix promotes the increase of T_3 compared to the value for the pure polymer, also suggesting that Li^+ ions compete with hydrogen bonding. It is also observed that the corresponding ΔH_{T_3} is almost constant ($\Delta H_{T_3} = 2\text{--}3 \text{ J g}^{-1}$) up to 17 wt % salt, and then it increases significantly reaching 30 J g^{-1} at 35 wt % salt. This result suggests the formation of long-range ordering at higher concentration, involving hard-segment hydrogen bonds.

Therefore, besides the comparison of our system with the TPU systems studied by other authors,^{9,13,40,41} the increase of the ΔH_{T_3} when the salt concentration increases corroborates the proposition that this third thermal event is associated with a hard-segment ordered phase.

The behavior of the three thermal events observed for the TPU(PTMG/PEG)/HMDI points to the same critical limit of concentration near 22 wt %. T_{g1} increases very slowly with LiClO_4 concentration and attains a plateau in the same composition region in which T_{g2} shows a slight increase, and ΔH_{T_3} also exhibits higher values. In addition, a distribution of a crystal-like phase was observed macroscopically for the 32 and 35 wt % systems. As will be demonstrated later (by Raman spectroscopy), this crystal-like phase is not precipitated LiClO_4 . Therefore, we can conclude that the TPU electrolytes exhibit a phase-separated morphology over the whole range of concentrations with an amorphous soft segment phase and a hard segment with short-range and long-range order. The higher concentrations showed phase segregation of the hard segment/salt crystals.

Ionic Interaction. As discussed above, the ion–ion interaction may be studied by using a Raman scattering technique, following the behavior of the ν_1 symmetrical stretching mode of anions, like ClO_4^- .²³ As the environment of ions is changed, their internal vibrational frequencies are affected. For identical ions in different environments (for example, in the form of free ions, ionic pairs, or multiple aggregates) the internal frequency

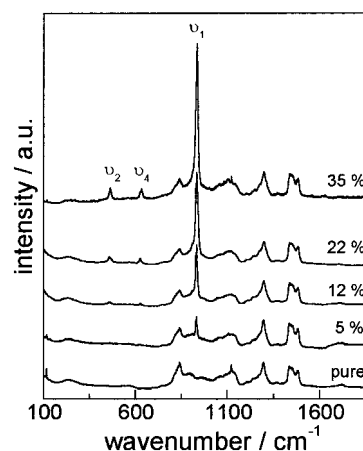


Figure 4. Normalized Raman spectra of the PU(PTMG/PEG)/ LiClO_4 system.

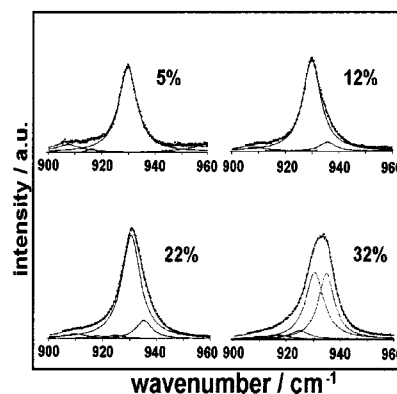


Figure 5. The Raman peak associated with the anion symmetric stretching mode for different PU(PTMG/PEG)/ LiClO_4 compositions fitted by the sum of Lorentzian lines.

of the ion splits in different frequencies corresponding to each specific environment.

The free anion ClO_4^- has T_d symmetry with four Raman-active normal modes of vibration $\nu_1(A_1)$, $\nu_2(E)$, $\nu_3(T_2)$, and $\nu_4(T_2)$.⁴⁴ The mean values of vibration frequency for these modes were deduced from individual values, obtained from the Raman spectra of LiClO_4 salt solutions in different aprotic solvents (DMSO, DMF, THF, MeTHF, THP):⁴⁴ $\nu_1(A_1) = 931 \text{ cm}^{-1}$, $\nu_2(E) = 458 \text{ cm}^{-1}$, $\nu_3(T_2) = 1100 \text{ cm}^{-1}$, and $\nu_4(T_2) = 624 \text{ cm}^{-1}$.

For the PU(PTMG/PEG)/ LiClO_4 electrolytes, the modes ν_1 , ν_2 , and ν_4 were found at 932, 463, and 633 cm^{-1} , respectively. Figure 4 illustrates the evolution of the intensity of these peaks as a function of increasing salt concentration. The ν_3 mode was not observed in the spectra, since it presents a very low Raman cross section. The spectra were normalized using the intensity of the Raman peak of the polyurethane at 1296 cm^{-1} as a reference. This peak is associated with the twisting of the C–H bonds,^{34,45} and it is not affected by the introduction of the salt.

The ion–ion interaction study was performed by a careful analysis of the ν_1 symmetrical stretching mode, since this mode is not degenerated and it is the most intense peak of the ClO_4^- anion. With increasing salt concentration, the evolution of the intensities of the peaks was observed and, in the particular case of ν_1 , the broadening and the splitting of the band was also followed. These effects are related to the formation of associated anionic species, in which the vibrational frequency is shifted to higher values compared to those for the free species.

Figure 5, which is an extract of the 930 cm^{-1} region from Figure 4, shows the corresponding band profile for the PU-

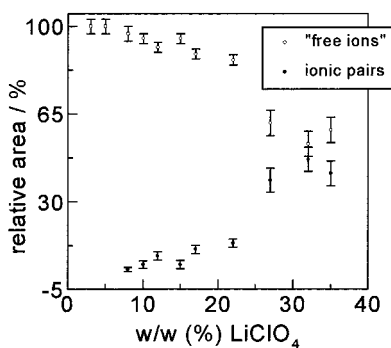


Figure 6. Relative amount of the different ionic associations identified in the PU(PTMG/PEG)/LiClO₄ Raman curves. The error was estimated for each set of experimental data by varying the fitting parameters.

(PTMG/PEG)/LiClO₄ systems at different compositions. A constant baseline was subtracted off the spectra in order to perform the fit analysis. For compositions up to 5 wt % LiClO₄, the observed band was fitted with a single Lorentzian at $\omega = 932 \text{ cm}^{-1}$, with line width $\Delta\omega = 8 \text{ cm}^{-1}$, attributed to “free” ions. The species named “free” ions can be seen as ions embedded in the macromolecular moieties or solvent-shared ion pairs.⁴⁴ For more concentrated samples, the ν_1 band could not be fitted by a single Lorentzian line with the same parameters used to fit the low composition electrolyte band, and therefore, a second Lorentzian line was introduced at $\omega = 937 \text{ cm}^{-1}$ and $\Delta\omega = 7 \text{ cm}^{-1}$. The second Lorentzian line was attributed to the presence of contact ion pairs,^{9,44} and its relative intensity is weak for concentrations smaller than 17 wt %. Figure 6 shows the relative area related to “free ions” and ionic pairs in the range of compositions studied. The error in the determined area was estimated for each set of experimental data to be less than 30 %, by varying the fitting parameters.⁴⁶ For compositions at 27 wt % salt and above, a significant increase of the relative concentration of ionic pairs was observed (Figure 6), which almost attains a plateau for the highly concentrated samples. Besides this high increase of contact ion pairs, no evidence of a significant concentration of aggregates was observed, detected in general through a line near 942 cm^{-1} . In the same way, no evidence of LiClO₄ precipitation emerged from a careful inspection of the concentrated samples. Raman lines with frequencies above 960 cm^{-1} are expected if higher aggregates⁴⁴ or salt micro-precipitates⁴⁷ are present. However, no line with $\omega \geq 960 \text{ cm}^{-1}$ was observed after several attempts to examining the macroscopic crystal-like phase observed for 32 and 35 wt %.

A band at about 924 cm^{-1} was observed for compositions of $\geq 22 \text{ wt } \%$ LiClO₄. This band was attributed to $2\nu_2$ ($2 \times 463 \text{ cm}^{-1}$),⁴⁴ and its relative intensity increased with increasing salt concentration.

The Raman results demonstrate the high ability of the TPU-(PTMG/PEG) to keep solvent-separated “free” ions as the majority species, in a wide range of salt concentration, as shown in Figure 6. This result also indicates a favorable structure from the ionic conductivity point of view. Ferry et al.⁹ have reported a rather lower dissolution ability of a TPU material, as the formation of higher aggregates was observed above 3 wt % salt. However, those authors studied a commercial TPU of PTMG with probably a high content of hard and aromatic segments.

The comparison of the DSC data and Raman results clearly indicates a transition region of concentration between 22 and 27 wt % salt in which a high content of ion pairs is formed (about 40%, in Figure 6) in addition to the T_{g1} plateau (Figure 3) and sensitive variations of T_{g2} and ΔH_{T3} (Table 1). The

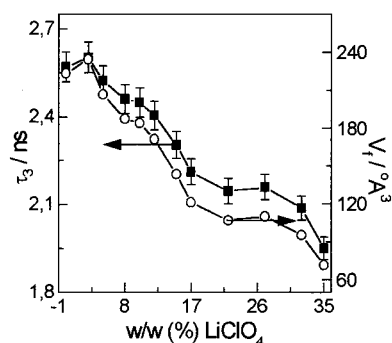


Figure 7. τ_3 and \bar{V}_f as a function of the concentration for the polyurethane/salt system, at 21 °C.

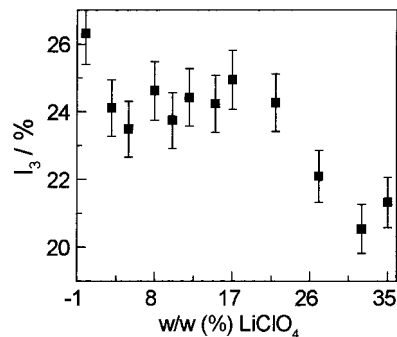


Figure 8. I_3 as a function of the concentration for the polyurethane/salt system at 21 °C.

Raman results also indicate that the crystal-like phase being formed in the highly concentrated electrolytes does not involve pure LiClO₄.

Average Free Volume. The results from positron annihilation spectroscopy (PALS) are summarized in Figures 7 and 8. Figure 7 shows the variation of the ortho-positronium lifetime (τ_3), and Figure 8 shows the variation of the o-Ps relative intensity (I_3), as a function of the salt concentration for the PU(PTMG/PEG)/LiClO₄ system.

As discussed in the literature, if no positron and/or positronium chemical reactions are present, as inhibition of Ps formation and quenching of o-Ps lifetime effects,^{32,48,49} according to the free volume model,²⁸ the PALS parameters τ_3 and I_3 may be related, respectively, to the mean radius of the free-volume cavities and to the relative concentration of holes present in the amorphous regions of polymer systems. According to the free-volume model of Ps formation,^{32,33} the o-Ps inside a free volume can be regarded as localized in an infinite spherical well of a thickness $\Delta R = R_0 - R$ and the annihilation rate ($1/\tau_3$) of o-Ps inside this electron layer is a constant equal to 2 ns^{-1} . In other words, the τ_3 can be directly correlated with the free volume radius, R (Å), by the following semiempirical equation, which has been proven to be widely applicable to a great variety of molecular solids:

$$\tau_3 = \frac{1}{\lambda_3} = \frac{1}{2} \left[1 - \frac{R}{R_0} + \frac{1}{2\pi} \sin\left(\frac{2\pi R}{R_0}\right) \right]^{-1} \quad (2)$$

The ΔR parameter = 0.165 ns has been determined empirically by fitting eq 2 to o-Ps annihilation data for molecular solids of known pore sizes. The spherical cavity volume is calculated through

$$\bar{V}_f = \frac{4}{3} \pi R^3 \quad (3)$$

The \bar{V}_f values shown in Figure 7 were calculated according to eqs 2 and 3. As shown in Figure 8, τ_3 decreases significantly with increasing salt concentration up to 22 wt % and then it remains approximately constant within the experimental error (± 0.05 ns). As the Li^+ and ClO_4^- ions are unable to promote inhibition or quenching effects,⁵¹ the observed decrease of the τ_3 values may be related to a decrease in the mean radius of the free-volume cavities of the amorphous phases, probably due to the coordination of the Li^+ ions with the solvating sites of the polymer, as observed for the PU(PEG/PPG)/ LiClO_4 system.¹⁹ The higher slope of the decrease in τ_3 is in the same concentration region in which T_{g1} shows a linear increase. In the same way, the stability of the T_{g1} and of the τ_3 values are in the same concentration region.

As shown in Figure 8, I_3 decreases initially, then it remains constant, within the experimental error, in the range 3–22 wt % of salt concentration, decreasing again at higher salt concentrations. The first decrease of I_3 from pure PU to the electrolyte system has been already discussed by Peng et al.¹⁷ as being associated with LiClO_4 diffusion toward the free-volume sites, which causes a reduction in the positronium formation probability. The coordination of Li^+ ion with the solvating sites is the driving force that governs the LiClO_4 diffusion.

Between 3 and 22 wt %, the increase of salt concentration does not produce any significant change of concentration of free volume (Figure 8) and only the free-volume size is modified (τ_3 decreases, Figure 7). For higher salt concentrations, I_3 exhibits a further pronounced decrease. This behavior suggests that, above 22 wt % of salt, the change in I_3 could be correlated with the morphological and Raman observations. The salt interactions with the hard segment that lead to the crystal-like phase segregation are clearer in the PALS results, which show a decrease in I_3 related to the free-volume concentration.

A complementary picture of the free volume in the materials can be obtained by inspection of the $\tau_3^3 I_3$ product, or the $V_f I_3$ product, as used by some authors.^{17,52} These products are proportional to the fraction of free volume, which is described by a simple semiempirical equation,^{18,30}

$$f = A I_3 V_f \quad (4)$$

where A is a constant for a particular material. At constant pressure, the fractional free volume varies as a function of temperature above T_g as described by the following equation:^{17,48}

$$f(T) = f(T_g) + \alpha_f(T - T_g) \quad (5)$$

where $f(T_g)$ is the free volume fraction at T_g and α_f is the thermal expansion coefficient for free volume, which is taken as the difference in the volume expansion of the samples above and below T_g . Since the determination of the absolute value of f by using eqs 4 and 5 requires the measurement of the constants using other methods, Peng et al.¹⁷ and Jean⁴⁸ have defined a “relative” fractional free volume (f_r). The important feature is not the absolute value of that parameter but its evolution when variables as composition and temperature are changed. For example, Peng et al.^{17,18} defined the f_r parameter as the $V_f I_3$ product, and they experimentally confirmed a quantitative correlation between the fractional free volume and conductivity above T_g , $\log[\sigma/\sigma(T_g)] = C_1[f(T) - f(T_g)]/f(T)$, in experiments in function of the temperature, for PEU– LiClO_4 complexes. These authors¹⁷ observed that the critical free volume required for the ion transport is much smaller than that required for

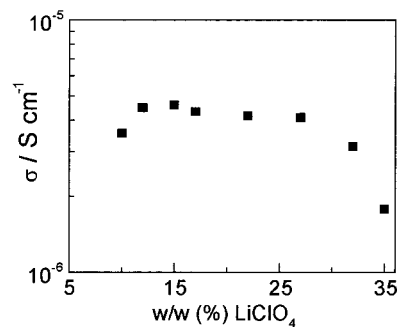


Figure 9. Concentration dependence of the total ionic conductivity (σ) for the PU(PTMG/PEG)/ LiClO_4 complex at 23 °C.

TABLE 3: Summary of PALS, Raman, and Conductivity Results for the Polyurethane/ LiClO_4

wt % LiClO_4	$\bar{V}_f I_3 / (\bar{V}_f I_3)_0$	“free” ion concentration (10^{20}) (atom cm^{-3})	conductivity (10^{-6}) (S cm^{-1})
5	0.85	7.4 (100%)	
8	0.89	11.4 (97.0%)	
10	0.85	14.0 (95.1%)	3.6
12	0.82	16.2 (91.6%)	4.5
15	0.76	21.0 (95.1%)	4.6
17	0.73	22.3 (89.0%)	4.3
22	0.67	28.0 (86.5%)	4.2
27	0.62	24.4 (61.4%)	4.1
32	0.55	25.0 (53.1%)	3.1
35	0.49	30.2 (58.7%)	1.8

polymer chain segment mobility. Besides that, they suggested that the ionic transport does not occur by itself, but segmental motion with associated carrier ions produces ionic transport, in accordance with the free-volume theory.

For the PU(PTMG/PEG)/ LiClO_4 system, the product $\bar{V}_f I_3$ of the electrolytes was calculated, normalized to the pure TPU. The values are shown in Table 3. This ratio $\bar{V}_f I_3 / (\bar{V}_f I_3)_0$ is proportional to the fraction of free volume in the samples and exhibits a continuous decrease in the overall range of salt compositions produced by the size or concentration of the free volume decrease.

Ionic Conductivity. The total ionic conductivity (σ) as a function of the salt concentration at room temperature is shown in Figure 9 for the PU(PTMG/PEG)/ LiClO_4 system. The system presents σ values of about $4 \times 10^{-6} \text{ S cm}^{-1}$ at 23 °C in a wide range of salt concentration from 10 to 27 wt %. This value is similar to that corresponding to a maximum conductivity obtained in a range from 1.5 to 5 wt % salt to LiClO_4 -doped TPU, synthesized containing PEG ($M = 1000$) as the soft segment and 22 wt % MDI–BDO as the hard segment.²⁰ In our range of salt concentrations, no maximum was observed, in agreement with results of other authors^{9,14,15} for a commercial TPU of PTMG/MDI/BDO.

Generally, the ionic conductivity can be expressed in terms of the mobility according to^{18,24}

$$\sigma = nq\mu \quad (6)$$

where μ is the mobility, n is the concentration of carrier ions, and q is the charge of the ions. This relation applies specifically to dilute, homogeneous electrolytes.²⁴ The presence of associations in highly concentrated electrolytes introduces an important factor to be considered.

The ionic diffusion coefficient is associated with the mobility by the Nernst–Einstein equation,

$$\mu = qD/kT \quad (7)$$

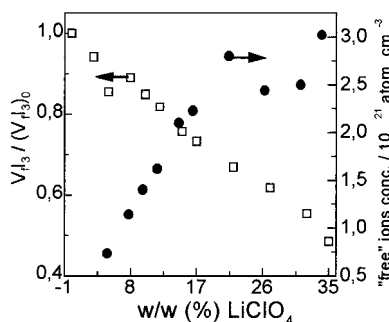


Figure 10. Relation between the $\bar{V}_{f3}/(\bar{V}_{f3})_0$ ratio, which is proportional to the fraction of free volume and the “free” ions concentration, as a function of the composition of the LiClO_4 -TPU, at room temperature.

where k is the Boltzmann constant and D is the diffusion coefficient. The free-volume theory proposed by Cohen and Turnbull⁵³ to describe the diffusion in polymer melts has been successfully used in modeling ion displacement in electrolyte polymers.^{18,24,26,27} The development of these ideas conducts to the establishment of a physical interpretation for the parameters of the phenomenological relationship [eq 1], which emphasizes the factor “average free-volume” as the determiner of the conductivity mechanism.

The observation of a sharp maximum is recurrent in conductivity isotherms for polymer electrolyte systems. In general, as salt concentration increases, the conductivity is raised 1 or 2 orders of magnitude (for example between 1 and 20 wt % for $\text{PEO}/\text{LiCF}_3\text{SO}_3$).⁵⁴ Following the maximum, the conductivity decreases in an almost similar way for concentrations higher than 30 wt %. This feature of polymer electrolyte isotherms can be explained by the opposite effects of increasing charge carrier concentration and decreasing free-volume fraction if we consider eqs 1, 6, and 7 and the Cohen–Turnbull theory as representative of the general behavior of polymer electrolytes.^{18,24,53} At lower concentrations, the increase of the number of charge carriers (Figure 10) dominates, and at high concentrations, the reduction of free-volume fraction (proportional to the ratio $\bar{V}_{f3}/(\bar{V}_{f3})_0$ on Table 3) takes precedence.¹⁷ Nevertheless, for the thermoplastic polyurethanes presented here, these two opposite effects produced a wide range of concentrations where no pronounced decrease of the maximum conductivity is observed. The experimental results concerning the fraction of the free volume related to the pure TPU and the number of charge carriers obtained considering the degree of association (Raman) are summarized in Table 3 and plotted in Figure 10 in which the opposite effects are clearly seen.

The broad maximum in ionic conductivity may be correlated to a less pronounced decrease of the free-volume fraction along with a larger increase in charge carrier concentration, when the TPU is compared to other electrolyte systems.^{17,54} This behavior has been observed for other TPU systems,^{9,11,14,15} although it was analyzed from a structural point of view in the present work.

For salt concentrations greater than 27 wt %, the conductivity finally decreases. This can be related (Figure 10) to the lower fraction of free volume no longer being compensated by a continuous increase of the charge carrier concentration.

Final Discussion and Conclusions

An experimental correlation between the opposite effects of free volume fraction decrease and charge carrier increase in the ionic conductivity was observed for TPU(PTMG/PEG)/ LiClO_4 when the concentration of salt was increased up to 35 wt %. The DSC study demonstrated the existence of a phase-separated

polyurethane with high segmental mobility in the soft phase and an increased degree of order in the hard phase when the concentration of salt is raised.

The low degree of association observed by Raman spectroscopy is responsible for a significant increase in charge carriers in the studied range of salt concentrations. However, a continuous decrease of the free-volume fraction (proportional to the ratio $\bar{V}_{f3}/(\bar{V}_{f3})_0$) should have produced a decrease in the conductivity more easily than was observed. The correlation observed cannot be considered unequivocal since the structural parameters obtained should be analyzed in the context of each technique and the extrapolation of the values for a comparison with the conductivity could be not obvious. Two main factors may be responsible for a nondirect and quantitative relation between the parameters in Table 3 and the measured conductivity. First of all, the time scale probed with Raman spectroscopy is several orders of magnitude faster (\sim picoseconds) than the typical time scales involved in conductivity measurements (microseconds to seconds), as discussed by Ferry et al.²⁴ This means that the ionic species observed by Raman spectroscopy could not be exactly the same ones involved in the conduction mechanism.²⁴

The second important feature is the nature of the free-volume dimension and relative concentration probed by Ps^{30} and, on the other hand, the characteristics of the dynamic reorganization of free volume, associated with the macromolecular chain, responsible for the conduction mechanism in an electrolyte.¹⁸ The numerical value, which can be related to the fractional free volume obtained by PALS, may not be a direct parameter to take into consideration when evaluating the conductivity process from a free volume point of view. This can be a consequence of the differences in interactions between the positron probe and the ionic species with the polymer matrix which are probably not negligible. However, it should be noted that Peng et al.,¹⁷ as previously mentioned, have established a relationship between ionic conductivity and a “relative fractional free volume” (I_3V_f), which efficiently relates their conductivity data, as a function of temperature for a fixed concentration, in a polyurethane network with LiClO_4 . Even considering the difficulties mentioned above, this work demonstrates that interesting insights about the conductivity behavior, with variations in the concentration of salt in an electrolyte polymer, can be obtained when the Raman and PALS structural results are presented and correlated.

The maintenance of conductivity near $4 \times 10^{-6} \text{ S cm}^{-1}$ up to 27 wt % of salt can be further analyzed by the evaluation of the dimensions for free volume shown in Figure 7. The \bar{V}_f decreases to near 110 \AA^3 when the concentration attains 27 wt %. A rough estimation of the critical free volume necessary for ion displacement in polymer electrolytes can be obtained using the value of the B parameter (eq 1). The TPU/ LiClO_4 materials studied here approach the order of magnitude of this critical free volume ($\sim 30 \text{ \AA}^3$) only after 32 wt %. At such concentrations, the conductivity starts exhibiting a slight decrease. Therefore, the average dimensions of the free-volume cavities seem to be high enough to permit the ionic migration in the overall range of salt concentrations.

Further investigation of the structure and ionic conductivity with temperature variations of the (PTMG/PEG) TPU is currently being carried out in order to obtain a more complete picture of the system behavior. The correlation between the critical free volume originating from the temperature dependence of the conductivity studies and the free volume dimension

obtained by PALS, relating to this material, will be published in a future communication.

Acknowledgment. The authors thank the Brazilian agencies PADCT, CNPq, FINEP, and FAPEMIG for financial support.

References and Notes

- (1) Armand, M. *Solid State Ionics* **1994**, *69*, 309.
- (2) Armand, M.; Sanchez, J. Y.; Gauthier, M.; Choquette, Y. *Electrochemistry of Novel Materials*; UCH Publishers: New York, 1994; p 65.
- (3) Fauteux, D.; Massuco, A.; Mclin, M.; Van Buren, M.; Shi, I. *Electrochim. Acta* **1995**, *40*, 2185.
- (4) Pernaut, J. M.; Silva, G. G. *Power Sources* **1995**, *55*, 93.
- (5) Berthier, C.; Gorecki, W.; Minier, M.; Armand, M.; Chabagno, J. M.; Rigaud, P. *Solid State Ionics* **1983**, *11*, 91.
- (6) Armand, M. B. In *Polymer Electrolyte Reviews 1*, 1st ed.; MacCallum, J. R., Vincent, C. A.; Elsevier: New York, 1987; Chapter 1.
- (7) Cheradame, H.; Le Nest, J. F. In *Polymer Electrolyte Reviews 1*, 1st ed.; MacCallum, J. R., Vincent, C. A.; Elsevier: New York, 1987; p 103.
- (8) Le Nest, J. F.; Gandini, A.; Cheradame, H. *Br. Polym. J.* **1988**, *20*.
- (9) Ferry, A.; Jacobsson, P.; Van Heumen, J. D.; Stevens, J. R. *Polymer* **1996**, *37/5*, 737.
- (10) Forsyth, M.; Meakin, P.; MacFarlane, D. R. *Electrochim. Acta* **1995**, *40*, 2339.
- (11) Watanabe, M.; Oohashi, S.; Sanui, K.; Ogata, N.; Kobayashi, T.; Ohtaki, Z. *Macromolecules* **1985**, *18*, 1945.
- (12) Seki, M.; Sato, K.; Yosomiya, R. *Makromol. Chem.* **1992**, *193*, 2971.
- (13) McLennagh, A. W.; Pethrick, R. A. *Eur. Polym. J.* **1988**, *24/II*, 1063.
- (14) van Heumen, J. D.; Stevens, J. R. *Macromol.* **1995**, *28*, 4268.
- (15) van Heumen, J.; Wiczorek, W.; Siekierski, M.; Stevens, J. R. *J. Phys. Chem.* **1995**, *99*, 15142.
- (16) Watanabe, M.; Nishimoto, A. *Solid State Ionics* **1995**, *79*, 306.
- (17) Peng, Z. L.; Wang, B.; Li, S. Q.; Wang, S. J.; Liu, H.; Xie, H. Q. *Phys. Lett. A* **1994**, *194*, 228.
- (18) Peng, Z. L.; Wang, B.; Li, S. Q.; Wang, S. J. *J. Appl. Phys.* **1995**, *77/1*, 334.
- (19) Forsyth, M.; Meakin, P.; MacFarlane, D. R.; Hill, A. J. *J. Phys. Condens. Matter* **1995**, *7*, 7601.
- (20) McLennagh, A. W.; Hooper, A.; Pethrick, R. A. *Eur. Polym. J.* **1989**, *25/12*, 1297.
- (21) Vallee, A.; Besner, S.; Prud'Homme, J. *Electrochim. Acta* **1992**, *37/9*, 1579.
- (22) Ferry, A.; Jacobsson, P.; Stevens, J. R. *J. Phys. Chem.* **1996**, *100*, 12574.
- (23) Torrel, L. M.; Schantz, S. In *Polymer Electrolyte Reviews 2*, 1st ed.; MacCallum, J. R., Vincent, C. A.; Elsevier: New York, 1989; Chapter 1.
- (24) Ferry, A.; Oradd, G.; Jacobsson, P. *J. Chem. Phys.* **1998**, *108/17*, 7426.
- (25) Silva, R. A.; Silva, G. G.; Pimenta, M. A. *Appl. Phys. Lett.* **1995**, *67/22*, 3352.
- (26) Souquet, J. L.; Duclot, M.; Levy, M. *Solid State Ionics* **1996**, *85*, 149.
- (27) Gray, F. M. *Polymer Electrolytes*, 1st ed.; RSC Materials Monographs, Connor, J. A., Ed.; The Royal Society of Chemistry, 1997.
- (28) Schader, D. M.; Jean, Y. C. *Positron and Positronium Chemistry, Studies in Physical and Theoretical Chemistry*; Elsevier: Oxford, New York, Tokyo, 1988; p 57.
- (29) Cheng, K. L.; Jean, Y. C.; Luo, X. H. *CRC Anal. Chem.* **1989**, *21*, 209.
- (30) Jean, Y. C. *Mater. Sci. Forum* **1995**, *175-178*, 59.
- (31) Yu, Z.; McGervey, J. D.; Jamieson, A. M.; Sinha, R. *Macromolecules* **1995**, *28*, 6268.
- (32) Tao, S. J. *J. Chem. Phys.* **1972**, *56*, 5499.
- (33) Eldrup, M.; Lightbody, D.; Sherwood, J. N. *Chem. Phys.* **1981**, *63*, 51.
- (34) Furtado, C. A.; Silva, G. G.; Pimenta, M. A.; Machado, J. C. *Electrochim. Acta* **1998**, *43/10-11*, 1477.
- (35) Braun, D.; Cherdron, H.; Kern, W. *Practical Macromolecular Organic Chemistry*; MMI Press: London, 1984; p 285.
- (36) Le Nest, J. F. Thesis, INP, Grenoble, 1985.
- (37) Le Nest, J. F.; Gandini, A.; Armand, M. *Electrochim. Acta* **1992**, *37* (9), 1585.
- (38) Kikegaard, P.; Eldrup, M.; Mogensen, O. E.; Pedersen, N. J. *Comput. Phys. Commun.* **1981**, *23*, 307.
- (39) Silva, G. G.; Lemes, N. H. T.; Fonseca, C. N. P.; De Paoli, M.-A. *Solid State Ionics* **1997**, 105.
- (40) Leung, L.; Koberstein, J. *Macromolecules* **1986**, *19*, 706.
- (41) Seymour, R.; Cooper, S. *Macromolecules* **1973**, *6* (1), 48.
- (42) Lee, H. S.; Wang, Y. K.; Hsu, S. L. *Macromolecules* **1987**, *20*, 2089.
- (43) Senich, G. A.; MacKnight, W. J. *Macromolecules* **1980**, *13*, 106.
- (44) Chabanel, M.; Legoh, D.; Tovaj, K. *J. Chem. Soc., Faraday Trans.* **1996**, *92/21*, 4199.
- (45) Papke, B. L.; Ratner, M. A.; Shriver, D. F. *J. Electrochem. Soc.: Electrochem. Sci. Technol.* **1982**, *129* (7), 1434.
- (46) Ferry, A. *J. Phys. Chem. B* **1997**, *101*, 150.
- (47) Leong, W. H.; James, D. W. *Aust. J. Chem.* **1969**, *22*, 499.
- (48) Jean, Y. C. *Microchem. J.* **1990**, *42*, 72.
- (49) Hodge, R. M.; Bastow, T. J.; Edward, G. H.; Simon, G. P.; Hill, A. J. *Macromolecules* **1996**, *29*, 8137.
- (50) Wang, C. L.; Maurer, F. H. *Macromolecules* **1996**, *29*, 8249.
- (51) Abbe, J. Ch.; Duplatre, G.; Maddock, A. G.; Talamoni, J.; Haessler, A. *J. Inorg. Nucl. Chem.* **1981**, *43*, 2603.
- (52) Hill, A. J.; Zipper, M. D.; Tant, M. R.; Stack, G. M.; Jordan, T. C.; Shultz, A. R. *J. Phys.: Condens. Matter* **1996**, *8*, 3811.
- (53) Cohen, M. H.; Turnbull, D. *J. Chem. Phys.* **1959**, *31*, 1164.
- (54) Robitaille, C. D.; Fauteux, D. *J. Electrochem. Soc.* **1986**, *133*, 315.